nature genetics

Periodic stripe formation by a Turing mechanism operating at growth zones in the mammalian palate

Andrew D Economou[1], Atsushi Ohazama[1], Thantrira Porntaveetus[1], Paul T Sharpe[1], Shigeru Kondo[2], M Albert Basson[1], Amel Gritli-Linde[3], Martyn T Cobourne[1] & Jeremy B A Green[1]

We present direct evidence of an activator-inhibitor system in the generation of the regularly spaced transverse ridges of the palate. We show that new ridges, called rugae, that are marked by stripes of expression of *Shh* (encoding Sonic hedgehog), appear at two growth zones where the space between previously laid rugae increases. However, inter-rugal growth is not absolutely required: new stripes of *Shh* expression still appeared when growth was inhibited. Furthermore, when a ruga was excised, new *Shh* expression appeared not at the cut edge but as bifurcating stripes branching from the neighboring stripe of *Shh* expression, diagnostic of a Turing-type reaction-diffusion mechanism. Genetic and inhibitor experiments identified fibroblast growth factor (FGF) and Shh as components of an activator-inhibitor pair in this system. These findings demonstrate a reaction-diffusion mechanism that is likely to be widely relevant in vertebrate development.

Regularly spaced structures, from vertebrae to hair follicles to the stripes on a zebrafish, are a fundamental motif in biology. A molecular mechanism by which these structures might be generated involving a two-component diffusing activator-inhibitor chemical (morphogen) pair was first proposed by the mathematician Alan Turing[1]. Experimental demonstrations of this mechanism *in vivo* are few and either do not identify both diffusible morphogens or do not exclude alternative mechanisms. In 1952, Turing proposed a simple model showing how the reaction between two morphogens diffusing through a tissue could produce self-regulating periodic biological patterns—the so-called reaction-diffusion model[1,2]. Simulations of reaction-diffusion replicate many biological patterns, including zebrafish stripes[3], mollusk shells[4], alligator teeth[5], digits of the limb[6] and feather and hair follicle spacing[7,8]. However, few systems where reaction-diffusion is implicated are amenable to the experimental perturbation necessary to fully test whether this model explains their behavior (reviewed in refs. 2,9). In particular, most of the literature relies on the simple resemblance of experimental results to computer simulations, without identifying the molecular components. In some instances, only one member of the minimal activator-inhibitor pair is identified[3,10]. Even where two or more molecular components are identified, alternative mechanisms are not addressed. For example, a clock-and-wavefront model has been implicated in vertebrate somitogenesis[11], whereas cell contact–meditated lateral inhibition—the inhibition by pattern elements of formation of identical pattern elements in order to establish minimum periodic spacing—regulates the spacing of microchaetae and bristles in *Drosophila melanogaster*[12]. The recent finding that contact-mediated lateral inhibition can apply even where the spacing is quite sparse[13] suggests that alternative mechanisms could underlie periodic patterns more often than previously thought. In particular, the role of reaction-diffusion mechanisms in spotted patterns, such as those of hair and feather follicles[7,8], may need to be re-evaluated in light of this lateral inhibition alternative.

Palatal rugae are periodic ridges on the hard palate of mammals that are involved in sensing and holding food[14]. Rugal patterning may be a sensitive indicator of environmentally or genetically caused congenital abnormality[15]. The number of rugae varies between species: pigs have 21 (ref. 16), humans 4 and mice 8 (ref. 14). Studies in the mouse[17,18] have shown that rugae, marked initially by *Shh* expression, appear sequentially during embryonic development. Ruga 8 appears first, and subsequent rugae appear in a growth zone just anterior to it, each interposed successively between ruga 8 and its predecessor, although the most anterior ruga, ruga 1, appears out of order (**Fig. 1a**,**b**). The mechanism by which this periodic pattern is generated is unknown. It has been speculated that a reaction-diffusion mechanism is responsible[17], but the regular spacing is also consistent with other mechanisms. Moreover, the out-of-sequence appearance of ruga 1, before rather than after ruga 2, is as yet unexplained.

To examine whether the addition of rugae is strictly associated with localized anteroposterior growth, we measured inter-rugal spacing of palates at successive days of mid-gestation (**Fig. 1c**). Measurements showed the greatest growth between ruga 8 and the ruga anterior to it (ruga 5 at embryonic day 13.5 (E13.5)), exactly where new rugae appear (**Fig. 1d**). Some growth between ruga 5 and ruga 4 indicated a growth zone slightly larger than reported[18], although this growth was insufficient to increase rugal spacing above the approximately 200-µm threshold required for new rugal appearance. In contrast, anteroposterior growth in the anterior palate where ruga 1 appears was even less than between the other rugae. Here, however, tissue at a >200-µm distance from ruga 2 was generated by medial growth (**Fig. 1e**). New *Shh* expression appeared in this new distal tissue, maintaining the

[1]Department of Craniofacial Development, King's College London, London, UK. [2]Graduate School of Frontier Biosciences, Osaka University, Suita, Japan. [3]Department of Oral Biochemistry, Sahlgrenska Academy at the University of Gothenburg, Göteborg, Sweden. Correspondence should be addressed to J.B.A.G. (jeremy.green@kcl.ac.uk).

Received 2 May 2011; accepted 29 December 2011; published online 19 February 2012; doi:10.1038/ng.1090

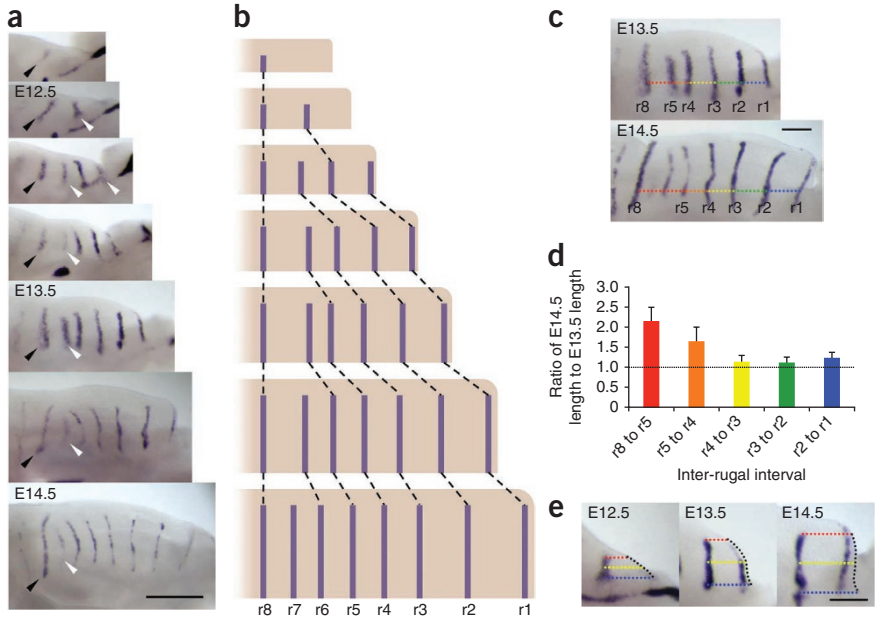

Figure 1 New rugal stripes appear in the palate at regions of growth. (**a**) *In situ* hybridization for *Shh* in the developing palatal shelves from mice at E12.0 to E14.5 (right, anterior; up, medial) showing the sequential addition of new rugae (white arrowheads) anterior to ruga 8 (r8; black arrowhead). Scale bar, 500 µm. (**b**) Schematic showing the sequential addition of rugae with growth. (**c**) Inter-rugal intervals measured at E13.5 and E14.5 along a line drawn from the point where the palatal shelf meets the posterior of the primary palate parallel to the midline of the head (dotted line). Scale bar, 200 µm. (**d**) Ratios of the lengths of the inter-rugal intervals at E14.5 and E13.5, indicating high levels of growth between r8 and ruga 5 (r5) and elevated growth between r5 and ruga 4 (r4), with little growth anterior to r4. Error bars, s.d. Colors in the histogram in **d** correspond to those for different inter-rugal intervals in **c**. (**e**) Growth anterior to ruga 2 (r2). Colored dotted lines show the orthogonal distance from *Shh* expression at r2 to the anterior shelf edge (black dotted line) at the base of the shelf (blue), medial edge of the stripe of *Shh* expression (red) and midway between (yellow). Growth in more medial regions correlated with the appearance of *Shh* expression at ruga 1 (r1) at the anterior edge. Scale bar, 200 µm.

association between growth-associated spacing and stripe appearance and explaining the latter's order.

The coupling of growth with the generation of new stripes is consistent with a simple fixed–inhibitory distance, lateral-inhibition mechanism (**Fig. 2a**) in which a stripe generates an inhibitor activity whose local level declines with distance from the stripe: as tissue grows and space between stripes increases, the inhibitor level falls below a threshold, and a new stripe can form. (Lateral inhibition in *Drosophila* takes this general form, although cellular mechanisms involving Notch-Delta signaling and cell-cell contact are not essential to it.) In this model, growth inhibition stops stripe addition. This is consistent with the correlation between the time of growth and the number of rugae among related rodent species[14]. We found that culturing palatal explants *in vitro* maintained mediolateral growth (indicating healthy tissue) but arrested anteroposterior growth (**Supplementary Fig. 1**). Unexpectedly, despite the lack of anteroposterior growth, new stripes

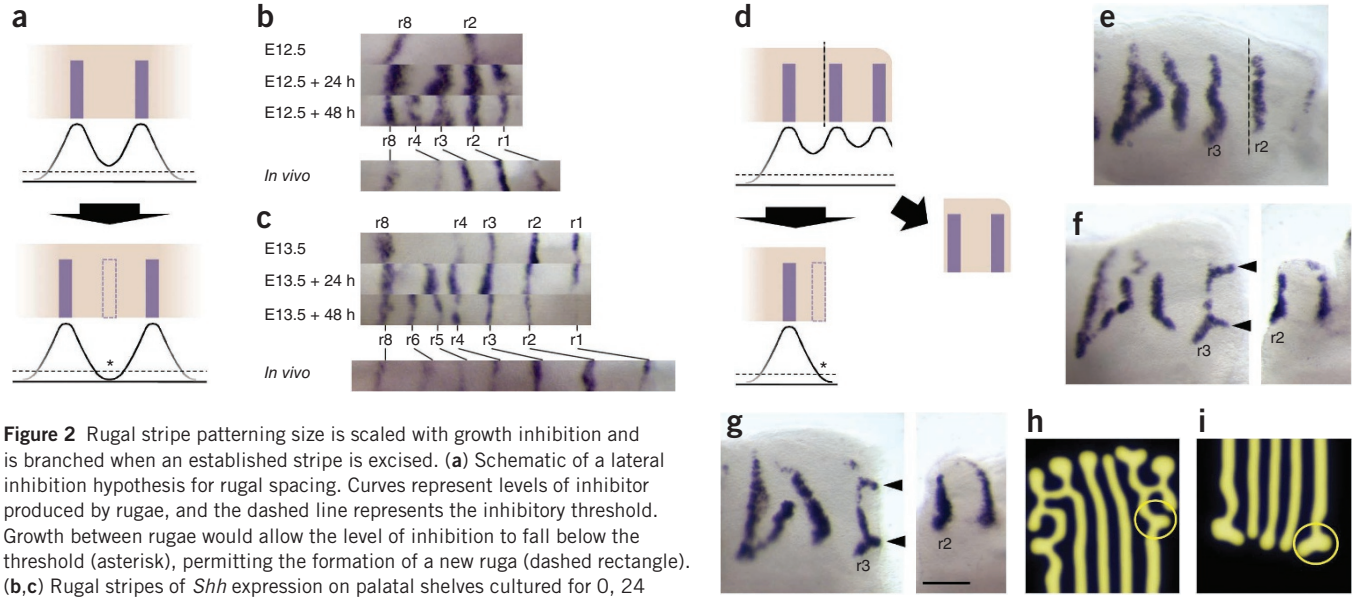

Figure 2 Rugal stripe patterning size is scaled with growth inhibition and is branched when an established stripe is excised. (**a**) Schematic of a lateral inhibition hypothesis for rugal spacing. Curves represent levels of inhibitor produced by rugae, and the dashed line represents the inhibitory threshold. Growth between rugae would allow the level of inhibition to fall below the threshold (asterisk), permitting the formation of a new ruga (dashed rectangle). (**b**,**c**) Rugal stripes of *Shh* expression on palatal shelves cultured for 0, 24 and 48 h after explant from littermates at E12.5 (**b**) and E13.5 (**c**), showing the addition of rugae without anteroposterior growth at closer spacing than the equivalent stripes *in vivo*. (**d**) Schematic representing the predicted effect of removing a ruga under a lateral inhibition model. Removing the anterior edge of the palatal shelf by cutting posterior to ruga 2 (vertical dashed line) removes inhibition from this ruga, allowing inhibition to fall below the threshold at the cut edge (asterisk) and leading to the formation of a new ruga (dashed rectangle). (**e**–**g**) Experimental results differed greatly from those predicted under a lateral inhibition model. Posterior palatal shelves cut adjacent to ruga 2 and cultured for 48 h with the anterior edge immediately fixed (**f**,**g**, two examples; right, uncultured anterior pieces) were analyzed by *Shh in situ* hybridization, which revealed branches to ruga 3 at curves in the ruga (black arrowheads), which was not seen in uncut controls (**e**). (Dashed line in **e** represents where the cut is in cut shelves.) (**h**,**i**) Branches to stripes were readily replicated in reaction-diffusion simulations generated using Turing equations as described[2]. Compare the pattern in circles in **h** and **i** (two examples) with those at arrowheads in **f** and **g**. For all specimens: right, anterior; up, medial.

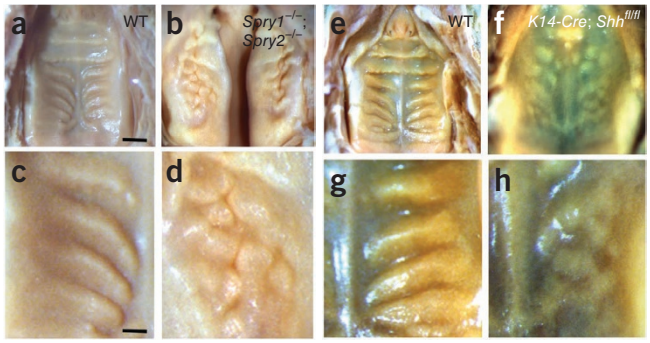

Figure 3 Sprouty and *Shh* loss-of-function mutants implicate FGF and Hedgehog signaling in rugal patterning. Palates of postnatal day 0 (P0) mice viewed from the oral side with the anterior side up. (**a**–**d**) Increased FGF signaling in *Spry1*$^{-/-}$; *Spry2*$^{-/-}$ mice resulted in disorganized and compacted rugae (**b**, detail in **d**) compared to wild-type (WT) animals (**a**, detail in **c**). Rugal phenotype can be distinguished despite cleft palate in these mutants. (**e**–**h**) Downregulation of *Shh* in *K14-Cre*; *Shh*$^{fl/fl}$ mice resulted in a similar phenotype of disorganized, compacted rugae (**f**, detail in **h**) compared to wild-type controls (**e**, detail in **g**). Scale bar in **a**, 1 mm (**a**,**b**,**e**,**f**); scale bar in **c**, 0.3 mm (**c**,**d**,**g**,**h**).

of *Shh* expression were still added in culture, but they appeared at smaller intervals than *in vivo* (**Fig. 2b**,**c**). This pattern scaling shows that growth and stripe generation are not rigidly coupled.

Pattern scaling (rather than truncation) also argues against a lateral inhibition mechanism of the type described above, although, if our method of growth inhibition somehow also causes reduced stripe inhibition, this model cannot be ruled out. We therefore tested a stronger prediction of this model, namely that removal of a stripe should lead to regeneration of a stripe near the cut edge because inhibition has been removed at this site (**Fig. 2d**). E13.5 palatal explants were cut immediately posterior to the ruga 2 (**Fig. 2e**). The anterior shelf was stained for *Shh* expression to confirm that the intended ruga was cleanly removed. When the posterior shelf was cultured for 48 h, new domains of *Shh* expression appeared anterior to ruga 3 in the form of 'branches', that is, stripes that branched anterior to ruga 3, extending toward the cut edge (**Fig. 2f**,**g**). Similar patterns were seen with cuts posterior to ruga 3 (data not shown). This result shows that the pattern is labile and that a lateral inhibition mechanism of the type described above does not apply, as new expression contiguous with existing expression is forbidden. Such expression can be explained if a self-propagating, diffusing activator is introduced. This is a definitive and distinguishing feature of Turing-type reaction-diffusion mechanisms. The branches emerged from slight convexities of the pre-existing stripe, producing junctions of expression lines at 120° angles (**Fig. 2f**,**g**), a typical manifestation of Turing-type reaction-diffusion patterning mechanisms (**Fig. 2h**,**i**). Branching or labyrinthine patterns are at the transition between stripes and spots achieved, for example, by reducing the basal levels of both activator and inhibitor[3]. Branches are inhibited by existing stripes but grow where neighboring stripes are absent (**Fig. 2h**,**i** and **Supplementary Fig. 2**).

Turing systems are defined by diffusible activator and inhibitor morphogens. Loss of the *Fgfr2* or *Fgf10* genes (encoding components of the FGF signaling pathway) results in a lack of palatal rugae[19,20], suggesting that FGF is an activator in this system. To address this possibility, we examined mice lacking the *Spry1* and *Spry2* genes that encode Sprouty intracellular antagonists of FGF signaling (these are compound mutant mice with the genotype *Spry1*$^{-/-}$; *Spry2*$^{-/-}$ (ref. 21)) as gain-of-function FGF signaling mutants. *Spry1* and *Spry2* are also FGF response markers and are expressed in palatal rugae during development[22] (**Supplementary Fig. 3** and data not shown). *Spry1*$^{-/-}$; *Spry2*$^{-/-}$ mice showed highly disorganized palatal rugae, including broader and ectopic ruga formation (**Fig. 3a**–**d**). Broader and disorganized rugae were prefigured by broader and disorganized *Ptch1* expression associated with epithelial thickening at earlier stages (**Supplementary Fig. 4**). Palates from these mutants bore many tightly packed bumps rather than well-spaced ridges, suggesting that rugal tissue was more widespread in addition to being more disorganized.

The rugal stripe marker *Shh* itself encodes a well-known morphogen, and the expression of its canonical target genes *Ptch1* and *Gli1* in and around the rugae show that it is actively signaling there (**Supplementary Fig. 3**), acting to prefigure the epithelial thickening of the rugae, even in the palates from *Spry1*$^{-/-}$; *Spry2*$^{-/-}$ animals (**Supplementary Fig. 4**). To address the role of *Shh* in rugal patterning, we investigated the effects of loss of Shh function by examining mice with a conditional deletion of *loxP*-flanked alleles of *Shh* in oral epithelial cells (*K14-Cre*; *Shh*$^{fl/fl}$ mice[23]). These mutants had highly disorganized rugae, including ectopic rugae formation (**Fig. 3e**–**h**). Disorganized rugae were prefigured by a similarly disorganized pattern of FGF signaling, as shown by *in situ* hybridization in which *Spry2* expression was coincident with thickened epithelium at E14.5 (**Supplementary Fig. 4**). The similarity of the phenotype from the conditional knockout of *Shh* to that of the *Spry1* and *Spry2* double null mutant suggests that Shh acts like Spry, functioning as an inhibitor of FGF signaling and of rugae formation in this system. Suggestively, in both mutant phenotypes, the patterns became fragmented, meaning that this system might be close to a stripe-spot transition that is well modeled by Turing equations[24]. However, despite the occurrence of Cre reporter activity in both the rugal placodes and the thin inter-rugal epithelium of *K14-Cre*; *ROSA26-lacZ* embryos (**Supplementary Fig. 5**), one cannot absolutely rule out the existence of a subset of cells that escaped or had delayed recombination events that could contribute to the uneven patterning. Thus, more direct tests of signaling pathway function were needed.

To analyze the roles of FGF and Shh more directly, we applied chemical inhibitors of these signals to explants in culture. Palatal explants were cultured with the FGF inhibitor SU5402

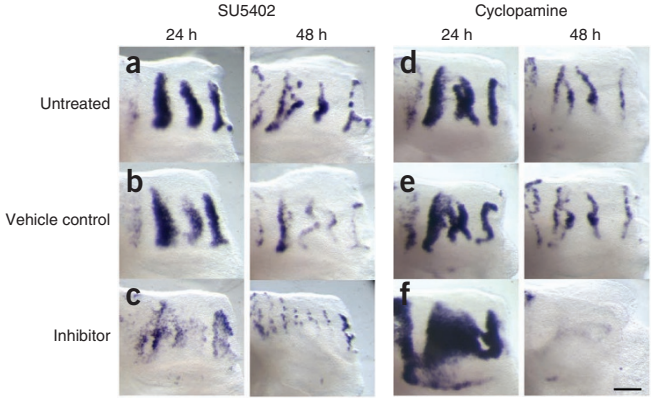

Figure 4 Inhibition of FGF and Hedgehog signaling in palatal explants shows their activatory and inhibitory roles, respectively, in rugal stripe maintenance. Pattern of rugae, visualized by *Shh in situ* hybridization in palatal shelf explants cut posterior to ruga 2 and cultured for 24 (left) and 48 h (right). (**a**–**c**) Explants cultured with the FGF inhibitor SU5402 showed reduced levels of *Shh* expression (**c**) relative to controls (**a**,**b**). (**d**–**f**) Explants cultured with the Hedgehog inhibitor cyclopamine showed increased levels of *Shh* expression after 24 h (**f**, left) relative to controls (**d**,**e**, left). Levels of *Shh* expression fell after 48 h in explants cultured with cyclopamine (**f**, right) compared to controls (**d**,**e**, right). All specimens: right, anterior; up, medial. Scale bar, 200 μm.

(JNDVEAXZWJIOKB-JYRVWZFOSA-N), the Shh signaling inhibitor cyclopamine (QASFUMOKHFSJGL-LAFRSMQTSA-N) or the Shh agonist purmorphamine (FYBHCRQFSFYWPY-UHFFFAOYSA-N). Exposing explants to SU5402, cyclopamine and purmorphamine and probing for *Spry2* and *Ptch1* expression confirmed that FGF and Shh signaling were inhibited or enhanced as expected for these reagents (**Supplementary Fig. 6**). After 24 and 48 h, SU5402-exposed explants showed substantially reduced *Shh* levels and a dispersed pattern of expression compared to controls (**Fig. 4a–c**). Culturing similar palatal explants with cyclopamine resulted in a pronounced broadening of *Shh* expression compared to controls at 24 h (**Fig. 4d–f**, left). Other markers of rugal patterning, namely *Spry2* expression and epithelial thickening, were similarly broadened (**Supplementary Fig. 7**). After 48 h in culture, there was almost no detectable *Shh* expression in palates exposed to cyclopamine, unlike in controls (**Fig. 4d–f**, right), suggesting a 'recoil' effect due to feedback control of expression. Treatment with the Shh-mimic purmorphamine[25] inhibited *Shh* expression, narrowing and eventually suppressing the stripes of *Shh* expression indicative of rugae (**Supplementary Fig. 7**), confirming that Shh signaling inhibits rugae. This result also shows negative feedback by Shh of its own expression. (One might speculate that the recoil effect is due to such feedback inhibition being triggered as increasing *Shh* synthesis after cyclopamine exposure overcomes the inhibition after 24 h.)

These results indicate that the FGF pathway is activatory and the Hedgehog pathway inhibitory in a Turing-type reaction-diffusion system that underlies the striped pattern that establishes and maintains the palatal rugae. It is highly unlikely that FGF and Shh are the sole diffusible morphogens in this system. The bone morphongenetic protein BMP4 is expressed in the rugal mesenchyme and regulates *Shh* expression in the palate[26], and mutations in *Sostdc1*, which encodes the Wise protein that interacts with BMP and Wnt morphogens, cause a rugal phenotype quite similar to those described in this work[18]. In addition, canonical Wnt signaling has been directly implicated in rugal patterning[27]. Size scaling also suggests additional components[28]. The interaction between these different pathways has the potential to be complex[29], but, although fuller understanding will require a more quantitative analysis, the work presented here indicates that this rectilinear system is amenable to experiments that reveal the character of the underlying mechanism. A recent analysis of the patterning of the regularly spaced cartilage rings in the trachea has implicated FGF10 and Shh signaling[30] (albeit without identifying them as a Turing activator and inhibitor, respectively). While other components (for example, other FGF and Wnt pathway proteins) have yet to be studied in that system, the involvement of these two pathways suggests that regular striped patterns may be similarly generated in multiple contexts in the mammalian body.

URL. ImageJ, http://rsbweb.nih.gov/ij/.

METHODS

Methods and any associated references are available in the online version of the paper at http://www.nature.com/naturegenetics/.

Note: Supplementary information is available on the Nature Genetics website.

ACKNOWLEDGMENTS

We would like to thank A. Lander and M. Cohen for useful advice on models, G. Martin (University of California, San Francisco) for the *Spry2* mutant mice, M. Kawasaki, Y. Otsuka-Tanaka and K. Kawasaki for assistance with *in situ* hybridization and M. Miodownik and M. Rubock for critical reading of the manuscript. This work was funded by a Medical Research Council (MRC; UK) grant (G0801154 to J.B.A.G. and M.T.C.).

AUTHOR CONTRIBUTIONS

A.D.E. performed palate measurements and explant experiments. T.P., A.O., P.T.S., M.A.B., A.G.-L. and M.T.C. constructed and analyzed the mouse mutants. S.K. performed the modeling. A.D.E., M.T.C. and J.B.A.G. designed the explant experiments and wrote the manuscript, with contributions from the other authors.

COMPETING FINANCIAL INTERESTS

The authors declare no competing financial interests.

Published online at http://www.nature.com/naturegenetics/.

1. Turing, A.M. The chemical basis of morphogenesis: a reaction-diffusion model for development. *Phil. Trans. R. Soc. Lond.* **237**, 37–72 (1952).
2. Kondo, S. & Miura, T. Reaction-diffusion model as a framework for understanding biological pattern formation. *Science* **329**, 1616–1620 (2010).
3. Asai, R., Taguchi, E., Kume, Y., Saito, M. & Kondo, S. Zebrafish *Leopard* gene as a component of the putative reaction-diffusion system. *Mech. Dev.* **89**, 87–92 (1999).
4. Meinhardt, H. *The Algorithmic Beauty of Seashells* 4th edn. (Springer-Verlag, 2009).
5. Kulesa, P.M. *et al.* On a model mechanism for the spatial patterning of teeth primordia in the alligator. *J. Theor. Biol.* **180**, 287–297 (1996).
6. Miura, T., Shiota, K., Morriss-Kay, G. & Maini, P.K. Mixed-mode pattern in Doublefoot mutant mouse limb—Turing reaction-diffusion model on a growing domain during limb development. *J. Theor. Biol.* **240**, 562–573 (2006).
7. Jiang, T.X., Jung, H.S., Widelitz, R.B. & Chuong, C.M. Self-organization of periodic patterns by dissociated feather mesenchymal cells and the regulation of size, number and spacing of primordia. *Development* **126**, 4997–5009 (1999).
8. Sick, S., Reinker, S., Timmer, J. & Schlake, T. WNT and DKK determine hair follicle spacing through a reaction-diffusion mechanism. *Science* **314**, 1447–1450 (2006).
9. Baker, R.E., Schnell, S. & Maini, P.K. Waves and patterning in developmental biology: vertebrate segmentation and feather bud formation as case studies. *Int. J. Dev. Biol.* **53**, 783–794 (2009).
10. Newman, S.A. & Bhat, R. Dynamical patterning modules: a "pattern language" for development and evolution of multicellular form. *Int. J. Dev. Biol.* **53**, 693–705 (2009).
11. Goldbeter, A. & Pourquie, O. Modeling the segmentation clock as a network of coupled oscillations in the Notch, Wnt and FGF signaling pathways. *J. Theor. Biol.* **252**, 574–585 (2008).
12. Axelrod, J.D. Delivering the lateral inhibition punchline: it's all about the timing. *Sci. Signal.* **3**, pe38 (2010).
13. Cohen, M., Georgiou, M., Stevenson, N.L., Miodownik, M. & Baum, B. Dynamic filopodia transmit intermittent Delta-Notch signaling to drive pattern refinement during lateral inhibition. *Dev. Cell* **19**, 78–89 (2010).
14. Pantalacci, S., Semon, M., Martin, A., Chevret, P. & Laudet, V. Heterochronic shifts explain variations in a sequentially developing repeated pattern: palatal ridges of muroid rodents. *Evol. Dev.* **11**, 422–433 (2009).
15. Ikemi, N., Kawata, M. & Yasuda, M. All-*trans*-retinoic acid-induced variant patterns of palatal rugae in Crj:SD rat fetuses and their potential as indicators for teratogenicity. *Reprod. Toxicol.* **9**, 369–377 (1995).
16. Pospieszny, N., Janeczek, M. & Kleć kowska, J. Morphology of the incisive papilla (*Papilla incisiva*) of pigs during different stages of their prenatal period. *EJPAU* **6**(1), Veterinary#04 (2003).
17. Pantalacci, S. *et al.* Patterning of palatal rugae through sequential addition reveals an anterior/posterior boundary in palatal development. *BMC Dev. Biol.* **8**, 116 (2008).
18. Welsh, I.C. & O'Brien, T.P. Signaling integration in the rugae growth zone directs sequential SHH signaling center formation during the rostral outgrowth of the palate. *Dev. Biol.* **336**, 53–67 (2009).
19. Rice, D.P., Rice, R. & Thesleff, I. *Fgfr* mRNA isoforms in craniofacial bone development. *Bone* **33**, 14–27 (2003).
20. Hosokawa, R. *et al.* Epithelial-specific requirement of FGFR2 signaling during tooth and palate development. *J. Exp. Zool. B. Mol. Dev. Evol.* **312B**, 343–350 (2009).
21. Simrick, S., Lickert, H. & Basson, M.A. Sprouty genes are essential for the normal development of epibranchial ganglia in the mouse embryo. *Dev. Biol.* **358**, 147–155 (2011).
22. Porntaveetus, T., Oommen, S., Sharpe, P.T. & Ohazama, A. Expression of Fgf signalling pathway related genes during palatal rugae development in the mouse. *Gene Expr. Patterns* **10**, 193–198 (2010).
23. Dassule, H.R., Lewis, P., Bei, M., Maas, R. & McMahon, A.P. Sonic hedgehog regulates growth and morphogenesis of the tooth. *Development* **127**, 4775–4785 (2000).
24. Shoji, H., Iwasa, Y. & Kondo, S. Stripes, spots, or reversed spots in two-dimensional Turing systems. *J. Theor. Biol.* **224**, 339–350 (2003).
25. Sinha, S. & Chen, J.K. Purmorphamine activates the Hedgehog pathway by targeting Smoothened. *Nat. Chem. Biol.* **2**, 29–30 (2006).
26. Zhang, Z. *et al.* Rescue of cleft palate in *Msx1*-deficient mice by transgenic *Bmp4* reveals a network of BMP and Shh signaling in the regulation of mammalian palatogenesis. *Development* **129**, 4135–4146 (2002).
27. Lin, C. *et al.* The inductive role of Wnt–β-catenin signaling in the formation of oral apparatus. *Dev. Biol.* **356**, 40–50 (2011).
28. Ishihara, S. & Kaneko, K. Turing pattern with proportion preservation. *J. Theor. Biol.* **238**, 683–693 (2006).
29. Ahn, Y., Sanderson, B.W., Klein, O.D. & Krumlauf, R. Inhibition of Wnt signaling by Wise (Sostdc1) and negative feedback from Shh controls tooth number and patterning. *Development* **137**, 3221–3231 (2010).
30. Sala, F.G. *et al.* FGF10 controls the patterning of the tracheal cartilage rings via *Shh*. *Development* **138**, 273–282 (2011).

ONLINE METHODS

Generation of embryos. Wild-type CD1 embryos were harvested, staged and stained by whole-mount *in situ* hybridization using established methods[31,32]. Measurement of palates before dissection and after staining confirmed that substantial shrinkage did not occur (data not shown). Mutant mice were generated from alleles previously described[23,33,34]. Phenotypes were determined for at least three embryos in all cases.

Explant culture. Palatal explants were cultured (37 °C, 5% CO_2) using the Trowell technique[26] in DMEM (Sigma) supplemented with 20 U/ml penicillin/streptomycin (GibcoBRL), 10% FBS (GibcoBRL), 50 mM transferrin (Sigma) and 150 μg/ml ascorbic acid (Sigma). For cutting and inhibitor experiments, serum-free Advanced D-MEM/F12 (GibcoBRL) supplemented as above was used. Medium was changed after 24 h for explants kept in culture for longer periods. Microdissections were performed with 0.1-mm tungsten needles. SU5402 (Calbiochem) was diluted in medium from a 10 mM stock solution in DMSO, and cyclopamine (Sigma) was diluted from a 20 mg/ml stock solution in ethanol. Experiments were repeated at least four times for each condition.

Imaging, measuring and simulations. Explants placed in a minimum volume of PBS in wells cut into 1% agarose were digitally imaged under a stereo dissecting microscope, and measurements were made using the ruler in ImageJ (see URL) calibrated with a micrometer slide. The dimensions of fixed material were within 8% of those of fresh, unfixed material (data not shown). Simulations of reaction-diffusion patterning were performed using Javascript[2] with the parameters $d_u = 0.03$, $D_u = 0.02$, $a_u = 0.1$, $b_u = -0.06$, $c_u = 0$, $F_{max} = 0.2$, $d_v = 0.06$, $D_v = 0.5$, $a_v = 0.1$, $b_v = +0$, $c_v = -0.2$ and $G_{max} = 0.5$.

31. Martin, P. Tissue patterning in the developing mouse limb. *Int. J. Dev. Biol.* **34**, 323–336 (1990).
32. Mootoosamy, R.C. & Dietrich, S. Distinct regulatory cascades for head and trunk myogenesis. *Development* **129**, 573–583 (2002).
33. Basson, M.A. *et al.* Sprouty1 is a critical regulator of GDNF/RET-mediated kidney induction. *Dev. Cell* **8**, 229–239 (2005).
34. Shim, K., Minowada, G., Coling, D.E. & Martin, G.R. *Sprouty2*, a mouse deafness gene, regulates cell fate decisions in the auditory sensory epithelium by antagonizing FGF signaling. *Dev. Cell* **8**, 553–564 (2005).

doi:10.1038/ng.1090